Annual Report for AOARD Grant FA2386-10-1-4059 "**Research Title**" Biological information processing in single microtubules

Date February 15, 2012

Name of Principal Investigators: Anirban Bandyopadhyay
- e-mail address : anirban.bandyo@gmail.com
- Institution : National Institute for Materials science
- Mailing Address : 1-2-1 Sengen, Main Building 815, Tsukuba
- Phone : +81-29-859-2167
- Fax : +81-29-859-2801

Period of Performance: 09/07/2011 – 08/07/2012 (Second year of 24 months progress report seeking one year further extension, as per option 0001)

Abstract: For the first time in the world we have isolated single brain microtubule reproduced it 200000 times faster than the conventional methods. This radio wave controlled technology to condense proteins adopting protein synchrony. We could take proteins from various samples and could generate synchrony in the water solution; this technology in future would help us in instant testing of inventory drug molecules. Until date it was not known why potential flux moves in the brain at a speed of 400km/hr, when electrons move only a few cm in years, we have found that through microtubule, solitons propagate at the speed of sound which explains mysterious high speed communication in the brain. We have defined what does it meant by information, everywhere we listen to the phrase "brain's information processing" but what does that visualization means? We have experimentally found and suggested it is "soliton".

Introduction: We started working on the brain microtubule way back in 2008, since, I understood that in the brain, neurons separated by 6 inches, synchronize, get phase and frequency locked and that is the source of enormous computability of the brain. However, no experimental evidence existed at that point of time. We became the first group in the world to study single microtubule electronics reliably and identify resonance band of these biological architectures, which was very essential to understand synchrony that would lead to phase and frequency lock conditions in the entire brain. Another problem bothered us for a long time; if we want to compute similar level of complex problems, we need 1000s of megawatts of energy; how brain does that using only 25 watt? We got an answer for that too, we discovered the soliton based information processing in the microtubule, which ensures dissipation less transport of information across the brain. Finally, that I desperately wanted to confirm was the potential of synchrony in brain computing, does brain execute non-linear frequency pulling to introduce simultaneity and drastically reduce the computing time? Yes, brain does that; we could even generate microtubules 200,000 times faster than the conventional methods, only if we triggered synchrony by applying a radio wave to the proteins in a heat bath.

Experiment: We felt three years back in 2008, that it was not sufficient just to try to build the artificial brain, when several fundamental mechanisms for brain operation was not clear—learning and memorizing like fundamental issues of our biological brain is a mystery. We started the microtubule research, extracted from neurons of human brain and several other living species. It was for the first time in the world; the electronics of the material that governed the evolution of living species for 3.5 billion years has been measured in a simple water beaker by exposing radio wave to the solution. The origin of high neurotransmission speed 400km/hr has been a mystery, we unraveled experimentally that soliton delivers the speed, and it defines the unit of information for brain computing. We have also resolved how two contradictory physical phenomena, memory and learning are realized

Report Documentation Page

Form Approved
OMB No. 0704-0188

1. REPORT DATE	2. REPORT TYPE	3. DATES COVERED
10 JUL 2012	**Final**	**15-06-2011 to 14-06-2012**

4. TITLE AND SUBTITLE	5a. CONTRACT NUMBER
Biological information processing in single microtubules	5b. GRANT NUMBER
	5c. PROGRAM ELEMENT NUMBER
6. AUTHOR(S)	5d. PROJECT NUMBER
Anirban Bandyopadhyay	5e. TASK NUMBER
	5f. WORK UNIT NUMBER
7. PERFORMING ORGANIZATION NAME(S) AND ADDRESS(ES)	8. PERFORMING ORGANIZATION REPORT NUMBER
National Institute of Material Sciences,1-2-1 Sengen Main Building, NIMS,Tsukuba 305-0047,Japan,NA,NA	**N/A**
9. SPONSORING/MONITORING AGENCY NAME(S) AND ADDRESS(ES)	10. SPONSOR/MONITOR'S ACRONYM(S)
AOARD, UNIT 45002, APO, AP, 96338-5002	**AOARD**
	11. SPONSOR/MONITOR'S REPORT NUMBER(S)
	AOARD-104059

12. DISTRIBUTION/AVAILABILITY STATEMENT

Approved for public release; distribution unlimited

13. SUPPLEMENTARY NOTES

14. ABSTRACT

By measuring fundamental electronic properties of a single brain microtubule, the researchers have found that it learns ~500 states by loss-less ferroelectric memory switching. They confirm that a single microtubule is a resonator with large quality factor, simultaneously operating with three distinct resonance bands, in the kHz, MHz and in the GHz frequency domain. It operates in the pico/femto-watt (1mV, 1pA) domain. They have underpinned its wireless communication and information processing potential that could unravel a hitherto unknown physical picture of the biological systems and trigger building of bio-inspired tunable multi-band resonators.

15. SUBJECT TERMS

microtubules, biological information processing

16. SECURITY CLASSIFICATION OF:			17. LIMITATION OF ABSTRACT	18. NUMBER OF PAGES	19a. NAME OF RESPONSIBLE PERSON
a. REPORT	b. ABSTRACT	c. THIS PAGE			
unclassified	**unclassified**	**unclassified**	**Same as Report (SAR)**	**7**	

simultaneously in the brain. Finally, we are able to track 3.5 billion years old evolution of living species by ultra-fast protein synchrony.
Porcine's brain, Tree, Algae extracted tubulins (Cytoskeleton, Denver, CO), were preserved at -80o C. To polymerize tubulin into microtubules, Microtubule cushion buffer (60 % v/v glycerol, 80 mM PIPES pH 6.8, 1 mM EGTA, 1 mM MgCl2) was added to General Tubulin Buffer (GTB, 80 mM PIPES pH 7, 1 mM EGTA, 2 mM MgCl2) and/or GTP solution. The mixture is added to 1 mg of tubulin. At 37o C, 10 mM tubulin leads to an uncontrolled growth of microtubule >100μm, we maintain this tubulin concentration for all experiments. GTP, TX (Taxol), VB (Vinblastine), K352 (Pironetin), N-termini, tau, CH (Colchicine) were optionally added to this solution individually or as a combination, produced microtubules were isolated for single nanowire measurement of resonance levels. Ultrasound power varied between pico-watt to femto-watt, if Mg2+ is not added, effect of ultrasound pumping is not observed, so Mg2+ is essential, GTP is not. Phase coherent signals were measured for all combinations of tubulin mixtures when placed in a heat-bath for pure ac pumping. The heat bath of Fig. 2a was placed inside the Raman measurement chamber and growth profile was measured with 532nm laser light from basic Raman spectrum switching between protein and microtubule nanowire shows convergence of Raman vibrations. We have ruled out possibilities of other physical processes detailed arguments in online text B. Rejection arguments: Rejection of DEP, rapid crystallization, ion-induced growth, self-assembly in the collapse of matter. For consistency, all figures in this paper are produced from porcine brain tubulin.

Results and Discussion: Here we describe the experimental results. Chemical route to synthesis microtubule is well established; instead, we develop radiofrequency-induced synchrony to fabricate microtubule-nanowires. Figure 2a shows the design of ac pumping and phase coherent signal capturing devices embedded together. The tubulin solution is added on this chip as a micrometer thick water film, the entire chip is covered with multilayered insulators for operating it as a heat bath. Within a millisecond of ac pumping, microtubule nanowire is produced, and an instantaneous burst of multiple phase coherent signals are captured in the coupled nano-probe circuit (experimental data is shown below Figure 2b scheme). Since protein oscillators are dissolved in water and the water molecules inside the film are continuously polarized before relaxation terminates25 by pumping alternating radiofrequency signal (MHz), proteins respond simultaneously in an orderly manner, which essentially forms the coupled-oscillator network.

Initially, the proteins oscillate with different phases and frequencies, then, due to delocalized energy transfer, attempt to reach equilibrium converge to a single frequency, initiating synchrony.17 Due to ac coupling through water, phase of all oscillators change in a sinusoidal manner, this is called normal modes of vibration, which squeezes to a single phase under strong coupling. If the phase and frequency of all participating proteins were not locked, coherent emission would disrupt immediately. However, the locked criterion sustains when all molecules are arranged in a particular symmetry inside the water film, from which one-step to reach global minima of entropy causes phase transition from liquid to the solid-state structure, which is microtubule. To prove this hypothesis, we pump tubulins without using GTP; then, we find microtubules at the bottom of the heat bath, but broken into small parts (~4μm) along the length, which suggests that even if GTP-hydrolysis that chemically constitutes microtubule14-16 is avoided completely, synchrony is sufficient to assemble proteins into a microtubular form (Fig. 2d). During this phase transition in water, a large number of oscillators switch simultaneously between two fixed energy states, which emit instantaneous burst of phase coherent signal. Unlike conventional assembly process, here reconstitution is extremely fast (105 times the growth rate without ac pumping and with GTP, Fig. 2c) and similar to known coherent collapse we detect ultra-low coherence rich signals, so, instead of assembly, we call it a collapse.

The growth rate of microtubule increases instantaneously as the ac signal is pumped, then

immediately it falls to zero (Fig. 2c inset), in contrast, for natural reconstitution without ac pumping, growth rate increases very slowly and then it remains constant. This suggests that ac pumping does not allow microtubule to grow beyond a certain length as coherent communication disrupts beyond that limit. Moreover, the average length of microtubule remains constant 25μm even if ac pumping is continued after growth rate falls to zero (Fig. 2c). Since average maximum length of microtubule is ~25μm inside a living cell, ultrasound induced non-coherent to coherent signal conversion mechanism and coherent communication among proteins should play a role in the microtubule growth.

Figure 2e,f shows a typical variation of average microtubule length with ac-pumping frequency in presence of GTP, which demands the necessity for several metastable states in the high radio-frequency region that triggers the synchrony of tubulin-assembly. The decomposition of length-frequency variation plot unravels seven such states in Figure S2, which requires laser like actions. The frequency of external ac pumping selects the particular structural symmetry of tubulin to resonate, therefore, six tubulin sites (+C-termini) observed in the microtubules of the living species and seven docking sites identified through molecular dynamics study of tubulin structure have one to one correspondences with these seven metastable states.

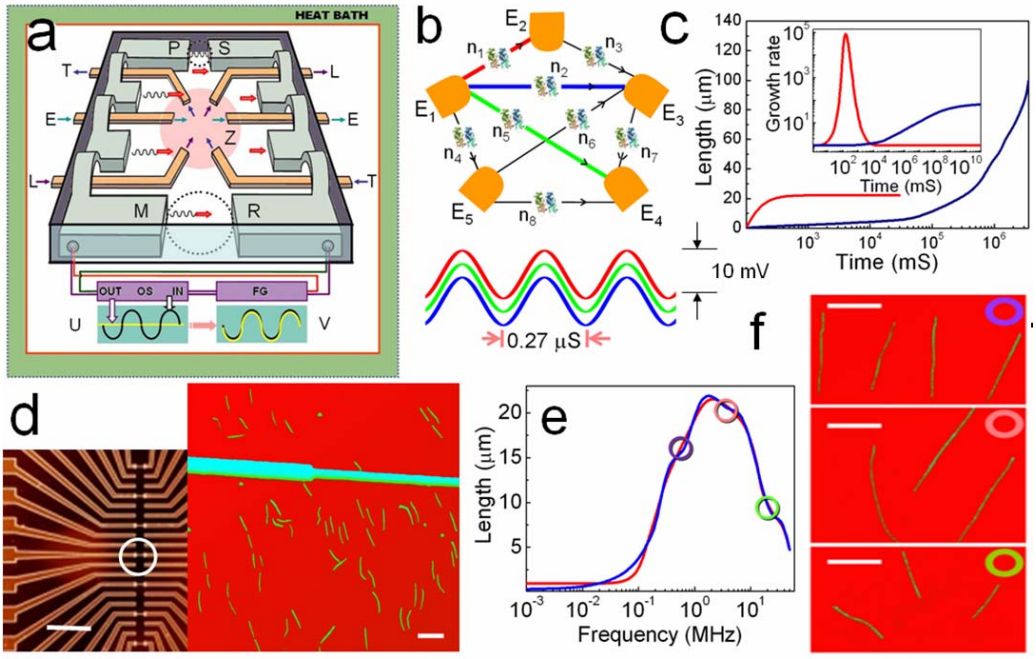

Figure 2. The synthesis of protein condensate: a. The heat bath. As FC forms, PS & MR (200nm gates) close, within ~100ms of Function Generator's (FG) triggering. Instantly, INput/OUTput U at OScilloscope converts to V. The L, E, T electrodes detect coherent signal in the electrically neutral circular region Z. **b**. Three coherent signals measured 1pico-Watt to 10femto-watt (bottom) during condensation (E-electrode (L,E,T), *n*-TD). **c**. Growth rate with GTP for MT when pumped (blue) and not pumped (red). Inset: MT's <L> with time-lapse when FC sets in (blue), in normal in-vitro reconstitution (red). **d**. SEM image of electrode array of heat bath (scale bar 300μm), circular region zoomed, AFM image of MT formed without using GTP (scale bar 4.5μm). **e.** MTs <L> plot, experimental (red) and theoretical (blue) against frequency ω. SEM image of heat-bath electrodes (scale bar 1mm, inset). **f**. AFM images of MTs (top-to-bottom) 500kHz(scale~7μm), 5MHz(scale~5μm) and 15MHz(scale~7μm) on SiO_2/Si (right).

A single microtubule's perfectly square or lossless hysteric current voltage (*IV*) characteristic at 10^{-6}Torr and in ambient conditions depicts a ferroelectric behavior, where hysteresis area is a function of maximum applied bias/current (Fig. 2a). Microtubule's ferroelectric memory was proposed based on its piezoelectric property only, we validate it experimentally.[27] Repeated cycles of temperature variation between 10K and 300K could not erase a ferroelectric state or bit encoded in a microtubule. Maximum ~500 bits could be written in an microtubule at a resolution of ~2 pA/bit. Only one bit could be written at a time and erased by an equal reverse field/current. Furthermore, since *IV* is square, all tubulin-dipoles reverse their direction at a fixed bias; there is minimal energy loss to write a bit and no energy is required to retain it. Figure 2b shows that ~1650 tubulin-dipoles switch to five distinct symmetries by reordering all dipoles simultaneously to process 5-bit information. Simulation shows that switching the dipole direction of a tubulin-dimer requires only ~1.7Å shifting of its charge center. All 40000 dimers could switch within ~200 pico-seconds, which is orders less than the time (~1μs) for electrons to cross the polymeric network of a tubulin-dimer (Figure 2c). Due to this difference, to an external observer, switching of all dipoles is 'simultaneous'.

Microtubule could switch between a metal and semiconductor since it's typical carrier density $\sim 10^{20}/cm^3$, is two orders more than the semiconductor and two orders less than a metal. Microtubule's solid-state dc resistivity is $\sim 1.3\times10^{-2}$Ohm.m for lattice A and $\sim 1.4\times10^{-3}$Ohm.m for lattice B, in liquid ~600Ohm.m,[11] similar to a semiconductor/insulator, but, similar to a ballistic conductor, the conductivity σ is independent of its length. The σ, measured using a source current (>10μA) by four-probe increases $\sim 10^7$ times the voltage-source-measured σ, the resistance becomes 39kΩ, 52kΩ, 104kΩ etc, which suggests that similar to carbon nanotube, microtubule's contact resistance is large. The ac resistance (lattice A~1MΩ, lattice B~80kΩ, at 1kHz, L=1μm) drops to the ballistic regime (A~39kΩ, B~6kΩ at 1MHz, L=1μm) if microtubule is exposed to a radio wave, and the frequency-resistance variation is again identical for any length, similar to a ballistic conductor.

Theoretically, microtubule is a topological insulator. To estimate possible Dirac points, we switch microtubule to a particular ferroelectric or ballistic state at 10K or 300K and then take it to 300K or 10K respectively (Fig. 3a). Apparently, the dc/ac resistivity (~10^{-9}Ohm.m at 20MHz) does not change with temperature in the range 10K-300K,[23-24], however, the encoded conductance (σ_E) is not truly constant; it consists of staircase-like jumps at various values of σ_S. If we plot σ_S, for different temperature scans, at least two adjacent σ_S states always appear, one above and one below σ_E (see methods C3), which suggests that the σ_S states act as spontaneously emerged protection-shields under thermal noise to switch microtubule back to σ_E, and they always appear in pairs. Higher is the σ_E, σ_S states are located nearer to σ_E; higher conductivity along the length of a microtubule transmits more electromagnetic energy, therefore, requires lower excess-heat adjustment, hence, σ_S states are closer to σ_E. Moreover, encoding a conducting state σ_E orients all tubulin-dipoles to a particular arrangement, therefore, to create equal σ_S spacing, all tubulin dipoles rotate equally at both sides of the angle of orientation at σ_E (Fig. 3c). The sum of σ_S and σ_E is always odd as required by a topological insulator. Simulation shows that topological phonon modes appear at the microtubule edges and the composition of σ_S and σ_E reflects a strong coupling

between the ferroelectric and the phonon modes.

To prove that $\sigma_S \rightarrow \sigma_E$ switching is associated with the spring action in the microtubule, we increased the heat gradient to 1K/minute, even under this extreme noise the conductivity oscillates periodically around σ_E (Fig. 3d). The periodicity changes with the heat gradient, which suggests that if the embedded spring expands/contracts, the fibonacci symmetry breaks, Dirac points splits, and the bands separate. However, if the symmetry is restored, the degeneracy appears, and the two-phonon bands touch at distant points. Thus, point-contact gates open/close during heat exchange process. Periodic oscillation denotes spontaneous splitting of σ_E; however, instead of random quantum jump, sinusoidal switching of microtubule through various σ_S levels suggests that the spring-like expansion/contraction is the final defense mechanism to survive σ_E or information. When heat gradient is decreased to a very low (0.1K/hour), σ_S levels shrink and eventually the quantized control re-appears.

To unravel the origin of quantum jump, we transmit thermal phonons along the Si-surface so that they propagate transversely across the microtubule. Atomic force image of microtubule at different biases show that the ripples on microtubule appear only at 3, 5 and 8 tubulin dimer rings apart (period). Dynamic electric field around microtubule interacts with the propagating thermal phonons; standing wave is produced acquiring symmetry exactly as reflected in the power spectrum of microtubule. Depending on threshold bias that wave transmits acquiring a periodicity 3,5 or 8; noise between two threshold signals is automatically filtered. Thus, cylindrical tubulin-grid works as a checkerboard where electron is restricted to a helical path, and the phonon modulates the pitch so moves perpendicularly along the length. The standing waves are seen to move to the outer circuit when both electrons and phonons are injected along the length. For a particular heat gradient, the height of standing waves reaching the external circuit periodically remains constant, depicting dissipation less transport of both electrons and phonons. Since, automatic noise correction is executed by topological symmetry and theoretical simulations suggest that in proteins solitons are the most feasible modes of dissipation less transport, the observed standing waves are the topological solitons.

When rapidly changing temperature or electrical noise oscillate the electronic/thermal solitons, then, the gates remain silent until noise magnitude matches the threshold for any one of the four allowed fibonacci paths. Energy distribution of phonon solitons of microtubule is located discretely between the energy levels of its electromagnetic solitons. Supplied energy is divided as a composition of electronic and thermal solitons (Fig. 4d). In the external circuit, we record added/subtracted conductivity σ_S, and if excess/less energy supplied through noise is dis-continued, additional point-contacts disappear path is closed.

Thus, continuous creation/destruction of point-contacts plays a major role in the cooperative management of purely mechanical phonon transport, and purely electromagnetic soliton transport. The protein structure spontaneously produces the electronic form of soliton, while, structural symmetry of 2D tubulin array is essential for the phonon-solitons. A harmony in opening/closing the gates for two kinds of solitons is achieved through the synchrony of dipoles, a remarkable dipolar rearrangement mechanism that enables it to shift the charge centers of all

tubulin-dimers simultaneously. Eventually, we observe an unprecedented transport of electrical energy that could naturally negate its associated mechanical vibrations.

Figure 2. Quantum nano-electro mechanical oscillator: Interference patterns
a. Quantum interference (QI) pattern of MT for dc source-drain with dc-gating (state |0>). **b.** Sinusoidal potential V is a function of pitch c~8nm (α&β tubulin, TD), and radius R~25nm. **c.** 3D dispersion plot (energy E vs. wave vector k); MPC-gating shows quantized charge tunneling only at threshold bias V. **d.** QI pattern at 20kHz, for ac source-drain with dc-gating (dispersion). **d.** QI pattern at 20kHz, for dc source-drain with ac-gating (state |1>).

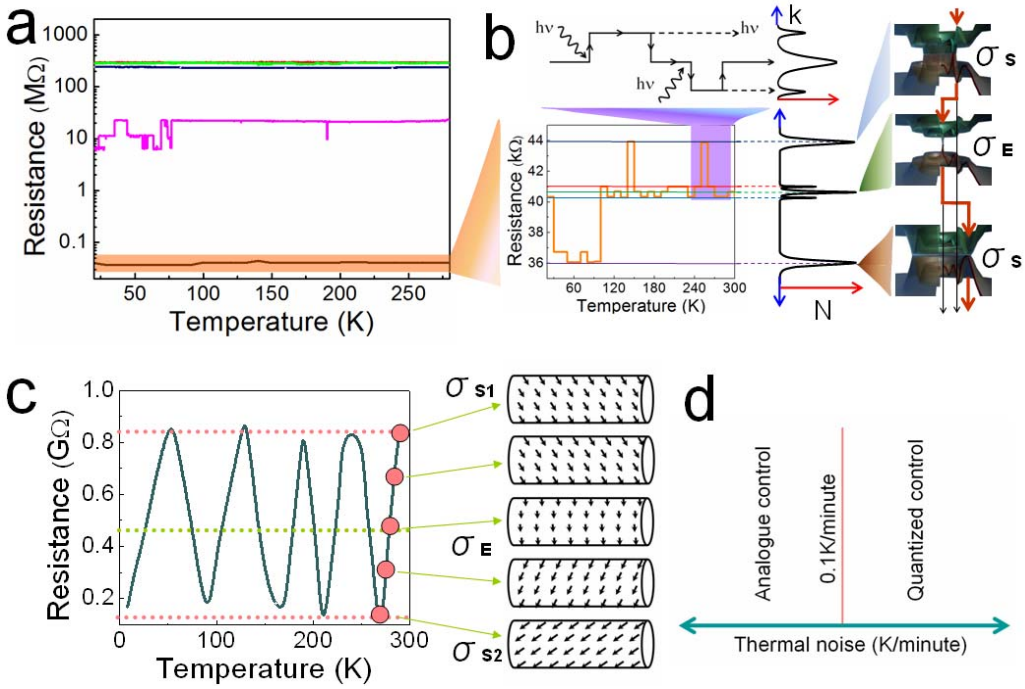

Figure 2.

List of Publications:

1. Computational myths and mysteries that have grown around microtubule in the last half a century and their possible verification S. Sahu, S. Ghosh, D. Fujita, A. Bandyopadhyay Journal of Computational and Theoretical Nanoscience (Special Issue) 8, 1-7 (2011), also selected for cover page
2. Radiofrequency induced ultra-fast condensation of microtubule and its length independent electronic properties S. Sahu, S. Ghosh, K. Hirata, D. Fujita, A. Bandyopadhyay Nature Materials (in press).

Lectures given in the international conferences and in the universities.

1. Remarkable electronic properties of a single Microtubule Google Mountain view campus, workshop on quantum biology 22 October 2010
http://www.youtube.com/watch?v=VQngptkPYE8

2. Practical computing with organic molecules Design and synthesis of a 3D nano brain, International symposium for Young Organic Chemists, Tsukuba, Japan March 1-3, (2011)

3. Quantum aspects of microtubule: Direct experimental evidence for the existence of quantum states in microtubule, Towards a science of consciousness May 2-8 (2011), Sweden

4. Electromagnetic energy of cells and microtubule: how microtubule research will revolutionize the human technologies, Czech Republic 1-3 July 2011

5. Remarkable technologies associated with microtubule, 29th February to 3rd March 2012, Rajasthan IIT.

6. Higher level information processing in the neuron as inspired by our microtubule research, Lucerne, Switzerland 30th March to 2nd April, 2012.

Lecture given in University of Arizona
http://streaming.biocom.arizona.edu/categories/?id=143

DD882: The invention disclosure process is underway. We hope by the end of the next year, we will be able to submit the invention disclosure with significant details.

This document may be as long or as short as needed to give a fair account of the work performed during the period of performance. There will be variations depending on the scope of the work. As such, there is no length or formatting constraints for the final report. Include as many charts and figures as required to explain the work. A final report submission very similar to a full length journal article will be sufficient in most cases.